Accepted Manuscript

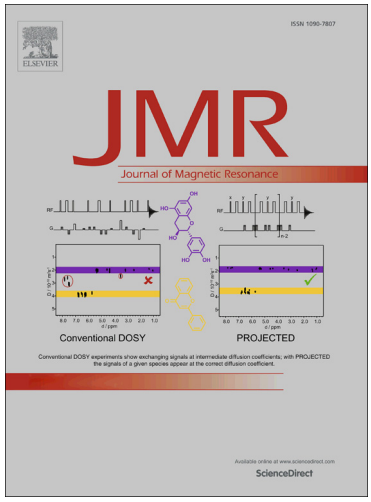

Room-Temperature Electron Spin Relaxation of Nitroxides Immobilized in Trehalose: Effect of Substituents Adjacent to NO-group

Andrey A. Kuzhelev, Rodion K. Strizhakov, Olesya A. Krumkacheva, Yuliya F. Polienko, Denis A. Morozov, Georgiy Yu. Shevelev, Dmitrii V. Pyshnyi, Igor A. Kirilyuk, Matvey V. Fedin, Elena G. Bagryanskaya

PII: S1090-7807(16)00117-8
DOI: http://dx.doi.org/10.1016/j.jmr.2016.02.014
Reference: YJMRE 5835

To appear in: *Journal of Magnetic Resonance*

Received Date: 4 November 2015
Revised Date: 4 February 2016

Please cite this article as: A.A. Kuzhelev, R.K. Strizhakov, O.A. Krumkacheva, Y.F. Polienko, D.A. Morozov, G.Y. Shevelev, D.V. Pyshnyi, I.A. Kirilyuk, M.V. Fedin, E.G. Bagryanskaya, Room-Temperature Electron Spin Relaxation of Nitroxides Immobilized in Trehalose: Effect of Substituents Adjacent to NO-group, *Journal of Magnetic Resonance* (2016), doi: http://dx.doi.org/10.1016/j.jmr.2016.02.014

Room-Temperature Electron Spin Relaxation of Nitroxides Immobilized in Trehalose: Effect of Substituents Adjacent to NO-group

Andrey A. Kuzhelev,[1,3] Rodion K. Strizhakov,[1,2] Olesya A. Krumkacheva,[2,3] Yuliya F. Polienko,[1,3] Denis A. Morozov,[1,3] Georgiy Yu. Shevelev,[3,4] Dmitrii V. Pyshnyi,[4] Igor A. Kirilyuk,[1,3] Matvey V. Fedin,[2,3,*] Elena G. Bagryanskaya[1,3,*]

[1]N. N. Vorozhtsov Novosibirsk Institute of Organic Chemistry SB RAS, Lavrentiev ave. 9, Novosibirsk, 630090, Russia; egbagryanskaya@nioch.nsc.ru

[2]International Tomography Center SB RAS, Institutskaya str. 3a, Novosibirsk, 630090, Russia; mfedin@tomo.nsc.ru

[3]Novosibirsk State University, Pirogova str. 2, Novosibirsk, 630090, Russia

[4]Institute of Chemical Biology and Fundamental Medicine, SB RAS, Novosibirsk 630090, Russia

Abstract

Trehalose has been recently promoted as efficient immobilizer of biomolecules for room-temperature EPR studies, including distance measurements between attached nitroxide spin labels. Generally, the structure of nitroxide influences the electron spin relaxation times, being crucial parameters for room-temperature pulse EPR measurements. Therefore, in this work we investigated a series of nitroxides with different substituents adjacent to NO-moiety including spirocyclohexane, cyclopentane, tetraethyl and tetramethyl groups. Electron spin relaxation times (T_1, T_m) of these radicals immobilized in trehalose were measured at room temperature at X- and Q-bands (9/34 GHz). In addition, a comparison was made with the corresponding relaxation times in nitroxide-labeled DNA immobilized in trehalose. In all cases phase memory times T_m were close to 700 ns and did not essentially depend on structure of substituents. Comparison of temperature dependences of T_m at T=80-300 K shows that the benefit of spirocyclohexane substituents well-known at medium temperatures (~100-180 K) becomes negligible at 300 K, because the conformational mobility of these groups becomes sufficiently high. Therefore, unless there are specific interactions between spin labels and biomolecules, the room-temperature value of T_m in trehalose is weakly dependent on the structure of substituents adjacent to NO-moiety of nitroxide. The issues of specific interactions and stability of nitroxide labels in biological media might be more important for room temperature pulsed dipolar EPR than differences in intrinsic spin relaxation of radicals.

I. Introduction

Pulsed dipolar Electron Paramagnetic Resonance (EPR) spectroscopy is nowadays being extensively used for nanoscale distance measurements in biomolecules, including large enough complexes of biological significance [1-7]. Although most of the experiments are usually done at cryogenic temperatures in frozen solutions, several recent advances opened up possibilities for application of the method at room/physiological temperatures as well [8-10]. Pulsed dipolar EPR spectroscopy, largely represented by Double Electron-Electron Resonance (DEER or PELDOR) [11-13], Double Quantum Coherence (DQC) [14,15] and a few other methods [16-20], relies on the measurement of dipole-dipole interaction between two spin labels. The accuracy of the measurement and accessible range of distances depend on the electron spin dephasing (or phase memory) time (T_m) of spin label.

Short T_m of most common nitroxide spin labels was a major complication for application of pulsed dipolar EPR at room temperatures (RT) until recently. The problem was partly remedied by implementation of new triarylmethyl (TAM) based spin labels allowing measurement of interspin distances up to ~4.6 nm [9]. In parallel, it has been demonstrated that the use of spirocyclohexane-substituted nitroxides in conjunction with immobilization in glassy trehalose allows measurement of interspin distances ~3.2 nm at RT [10]. Although T_m of TAM-based labels is still superior compared to nitroxides, there are certain advantages of using nitroxides for short-distance measurements at RT, since their spin-labeling strategies are much better developed and their availability is at the moment much broader.

The first RT distance measurement in nitroxide-labeled protein relied on two important advances [10]. First, spirocyclohexane-substituted nitroxide was used instead of more common tetramethyl-substituted one; the authors notice that DEER measurements were only possible for the former one due to noticeably longer T_m time [10,21,22]. Second, immobilization in trehalose was implemented to prevent averaging of dipolar interaction by motion of spin-labeled protein. Trehalose recently attracted huge attention as immobilizing medium due to its cryoprotective properties and ability to mimic water solution by creating hydrogen bonding networks [23-25]. Therefore, the use of trehalose for immobilization and advanced nitroxides for spin labeling appears to be a promising approach for RT distance measurements.

In this work we investigated a series of nitroxides with different substituents adjacent to NO-moiety (spirocyclohexane, spirocyclopentane, tetraethyl and tetramethyl groups) in order to find structure/property relations and establish further routes of optimization for RT distance measurements. Surprisingly, the dependence of T_m on structure of substituents adjacent to NO-moiety was not significant at RT. This was further elaborated by studying temperature dependence of T_m and allowed more general conclusions and recommendations for future studies.

II. Results and Discussion

II.1. Structure of studied nitroxides

Figure 1 shows chemical structures of studied nitroxides of piperidine (**2a,b**), pirroline (**1**, **2c,d**), pyrrolidine (**3**), imidazoline (**4b**, **5b**, **6b**) and imidazolidine (**4a**, **5a**, **6a**) series with different bulky substituents adjacent to NO-moiety including tetramethyl (**1**), tetraethyl (**4a,b**), bis-spirocyclohexane (**2a-d**), bis-spirocyclopentane (**3**), diethyl and spirocyclohexane (**5a,b**), diethyl and spirocyclopentane (**6a,b**) fragments.

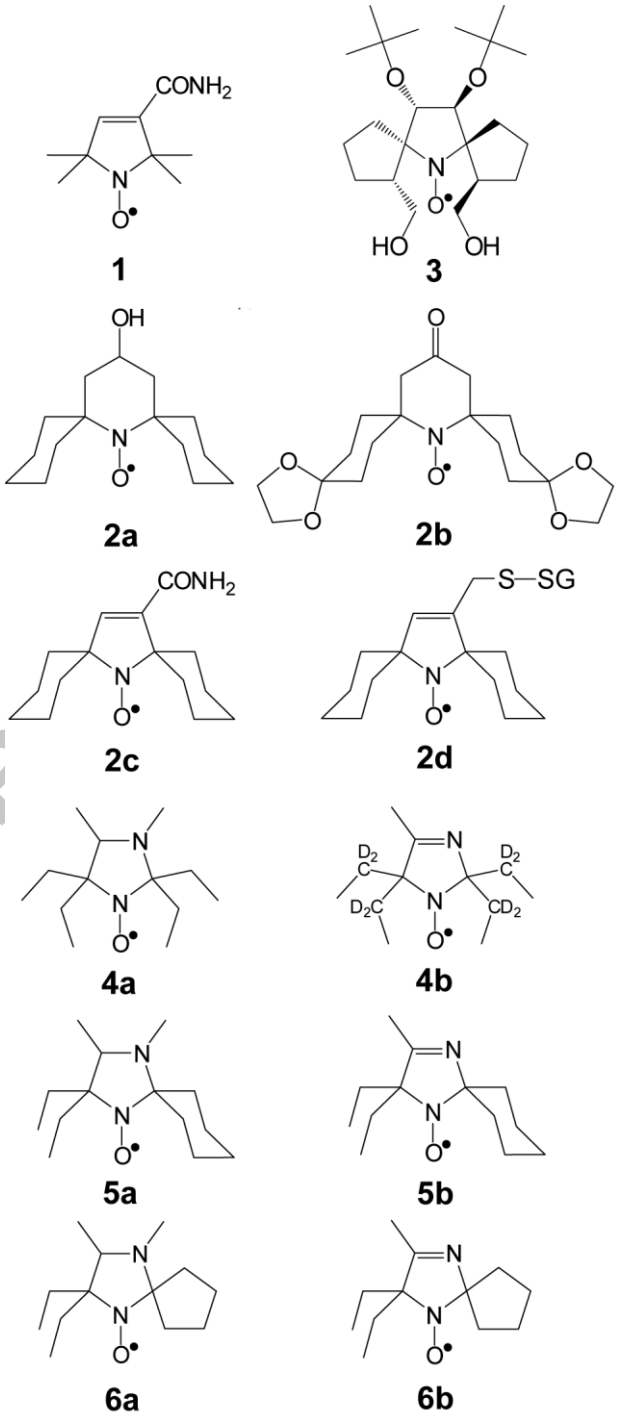

Figure 1. Structure of studied nitroxides.

The variety of these radicals allows us to investigate electron spin relaxation depending on type of radical as well as on the structure of bulky substituents. If the rotational motion of radical is hindered (as is the case in glassy trehalose), the primary relaxation mechanisms are (i) modulation of ^{14}N hyperfine interaction (HFI) anisotropy of NO group by librational motion, and (ii) modulation of HFI with other nuclei of radical by rotation of corresponding groups (e.g. rotation of tetramethyl groups in **1**). We considered both symmetric and asymmetric structures with combined cyclic/acyclic substituents. Cyclopentane and cyclohexane rings differ by rigidity and thus might induce contribution to T_m in different extent. In addition, T_m might depend on the amount of remaining water in the vicinity of NO group. In this regard, compound **3** represents radical with hydrophilic OH-groups, for which one expects the largest concentration of H_2O molecules close to NO moiety. Compound **2d** represents radical attached to glutathione (GSH), as a simple example of attachment to a small biomolecule.

II.2. Immobilization in trehalose evidenced by CW EPR

All studied radicals were prepared in glassy trehalose as described in Experimental Section below. In order to demonstrate that the immobilization is achieved we have measured CW EPR spectra of all samples at RT and simulated them using solid-state powder pattern. Four representative spectra for different groups of radicals are shown in Figure 2, whereas the rest of the data for other radicals is given in Supporting Information (SI). Spectral shapes correspond to the essentially immobile radical, i.e. the rotational motion is strongly suppressed. At the same time, simulations using solid state powder pattern do not allow good enough agreement in every case (Figure 2 and SI), indicating that the librational motions are clearly present. This follows from suppression of A_{zz} components compared to theoretical predictions, as well as by generally better agreement with simulations at 80 K compared to 300 K, since librations are more intensive at higher temperature (see SI for details).

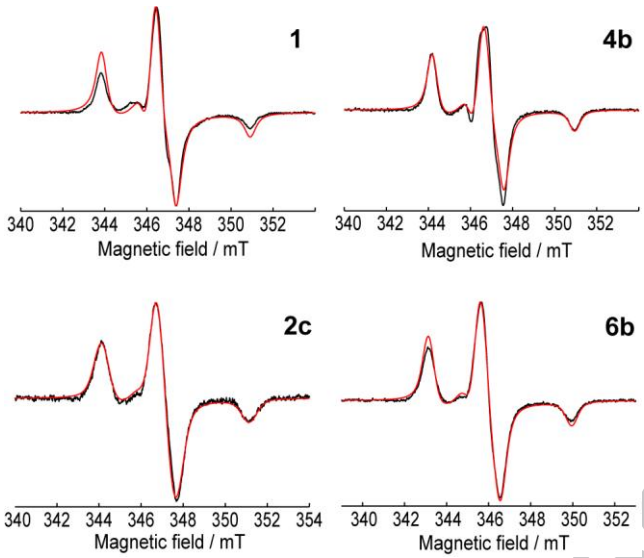

Figure 2. X-band CW EPR spectra of studied samples at room temperature (black) and corresponding simulations (red).

II.3. Relaxation times of free nitroxides at RT

As described in Experimental Section below, we used two-step drying procedure: mild drying (10^{-3} bar for 2 hours) and extensive drying ($3.5{\cdot}10^{-9}$ bar for 24 hours after mild drying). Relaxation times at RT were measured after each step (see Table 1). We have noticed that T_m is quite sensitive to the extent of drying, although not for every radical. At the same time, T_1 values were found similar after each step of drying. It has been shown that the concentration of remaining water in glassy trehalose has a significant influence on the EPR spectra and low-temperature relaxation rates [23, 24]. Evacuation at 10^{-3} bar results in concentration of water in trehalose being 7% [10]. Unfortunately, we could not determine the concentration of water remaining after evacuation at $3.5{\cdot}10^{-9}$ bar, but obviously it could only decrease compared to evacuation at 10^{-3} bar. As a result, one expects better immobilization of radical and further suppression of relaxation mechanisms. Still, Table 1 shows that extensive evacuation changes T_m relaxation times by no more than ~15% for most of the radicals, with the exception for radical **3** exhibiting ~22% change of T_m. Indeed, one would expect that the OH-groups in the structure of **3** should lead to the largest amount of H_2O molecules remaining in the vicinity of NO group.

Table 1. Electron spin relaxation times T_m and T_1 measured at X-band for studied radicals in dried trehalose at RT. The results are given for two drying conditions, indicated by different pressure during evacuation and described in more detail in the text. Accuracy of T_m and T_1 measurements is approx. 40 ns and 1 μs, respectively.

Radical	T_m, ns	T_m, ns	T_1, μs
	10^{-3} bar	$3.5 \cdot 10^{-9}$ bar	
1	625	735	12
2a	660	750	17
2b	680	730	17
2c	740	800	21
2d	610	630	22
3	575	730	30
4a	550	680	18
4b	650*	650*	14
5a	570	640	18
5b	630	740	16
6a	610	655	23
6b	630	730	16

*strong deuterium modulation allows rough estimation (±80 ns) only

Despite these relatively small effects, evidently, the T_m values of all radicals immobilized in trehalose are roughly 700 ns and do not demonstrate pronounced dependence on the structure of substituents adjacent to NO-moiety. At the same time, T_1 varies depending on structure between 12 μs for **1** and 30 μs for **3**. The T_m relaxation curves are slightly better described by biexponential decay with approximately equal weights and characteristic times ~400 and ~900 ns, however for simplicity of comparison Table 1 reports the result of monoexponential analysis (for rigorous biexponential treatment see Supporting Information). Note also that T_m noticeably depends on the spectral position (see Supporting Information); all values reported in Table 1 were obtained at the absolute maximum of the spectrum. In fact, all other spectral positions demonstrate shorter T_m values, as is quite typical for relaxation induced by librations of nitroxide [26,27,[28]].

No noticeable dependence of T_m on magnetic field was found during X- and Q-band measurements. For instance, for two representative radicals **1** and **2c** the values of T_m 720±40 ns and 740±40 ns were obtained at Q-band at the spectral maximum, respectively. Obviously, these values are similar to those reported in Table 1 within experimental accuracy.

Note that similarity of T_m values found for common tetramethyl-substituted nitroxide and spirocyclohexane-substituted one disagrees with the results of Ref.10, where noticeable improvement was reported for spirocyclohexane-substituted spin label (920 ns vs. 550 ns for tetramethyl-substituted one) in glassy trehalose at RT. In order to understand the reasons for these differences and underlying relaxation mechanisms we investigated temperature dependence of T_m in glassy trehalose for these two types of radicals.

II.4. Temperature dependence of T_m for free nitroxides

Figure 3 shows temperature dependences of T_m and T_1 for two representative radicals **1** and **2c** in trehalose. The shapes of T_m vs. T dependence (Fig.3a) are generally similar compared to the trends observed in frozen solutions (see e.g. Refs.21,29). Tetramethyl-substituted radical demonstrates drastic acceleration of phase relaxation ($1/T_m$) at T>100 K as rapid rotation of methyl groups becomes thermally-activated; at T>140 K this rotation becomes fast enough for averaging the HFI anisotropy, leading to some decrease of phase relaxation; finally, at T>220 K librational motion of NO group governs phase relaxation and its rate continues to increase with the temperature [30,31]. Contrary to tetramethyl-substituted radical, no bell-like shape is observed for spirocyclohexane-substituted radical, and only an increase of $1/T_m$ due to librations of NO group begins above ~170 K. Temperature dependence of $1/T_1$ is similar for both radicals and generally similar to that obtained in frozen solutions.

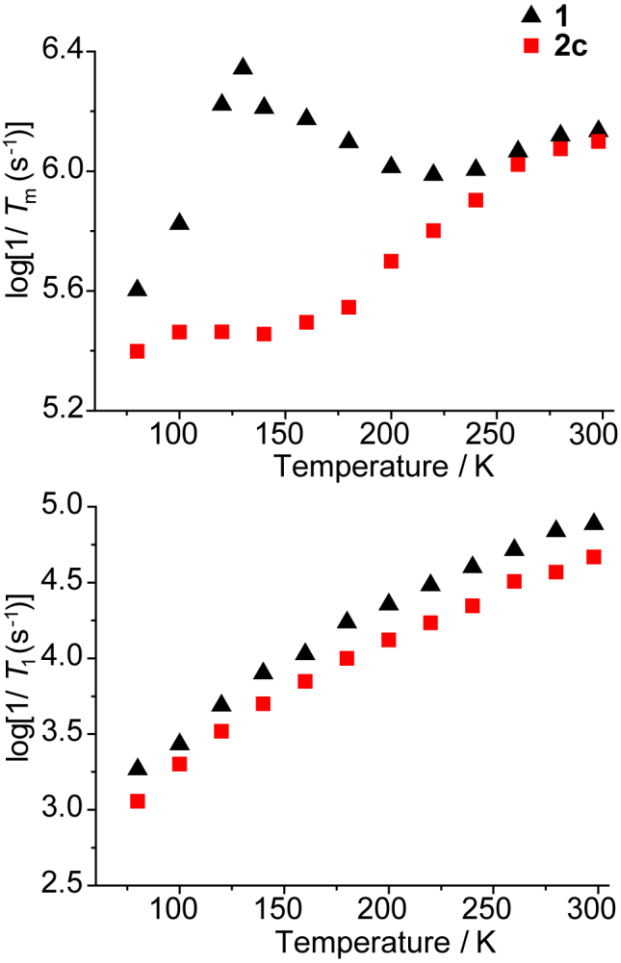

Figure 3. Temperature dependence of T_m (a) and T_1 (b) for **1** and **2c** in trehalose measured at X-band.

Note, remarkably, at room temperature the difference in $1/T_m$ between free **2c** and **1** becomes very small. At the same time, based on the study of spin-labeled protein, Ref.10 suggests

that there is a noticeable benefit of using spirocyclohexane-substituted spin labels compared to common tetramethyl-substituted ones. This disagreement can be reconciled assuming, very generally, that there are specific interactions of spin labels with the protein studied in Ref.10, and such interactions are different for the two types of labels. To elaborate on this hypothesis, at least to some extent, we have also compared two types of spin labels attached to oligonucleotide and immobilized in trehalose.

II.5. Relaxation times of nitroxides attached to DNA at RT

We have synthesized three DNA duplexes spin-labeled by pairs of tetramethyl- or spirocyclohexane-substituted nitroxides (Fig.4). Note that similar DNA duplexes were investigated in our previous work [32] (see this reference for structural details). The sample preparation approach used for free radicals turned out to be damaging for the structure of duplex, which partly "frayed" at its ends during water drying from trehalose [33-35]. This clearly follows from DEER/PELDOR data differing in trehalose compared to water solution [32] (more details in Supporting Information). However, for the purpose of the present work, such systems are still useful for investigation of spin relaxation of label attached to oligonucleotide.

Table 2 shows room-temperature relaxation data for three spin-labeled DNA systems in trehalose. The spin labels used are most close to **2c** and **1**, studied in trehalose vs. temperature in previous section. Remarkably, T_m value of spirocyclohexane-substituted label increased compared to **2c** radical (Table 1), whereas T_m of tetramethyl-substituted label remained close to that of **1**. In addition, we verified the effect of linker on T_m of tetramethyl-substituted label and found that more rigid NH linker leads to prolongation of phase relaxation. Both observations imply that the interaction with biomolecule is important (as was also found by us recently in Ref.32), and this interaction depends on the type of radical and linker used and, of course, strongly depends on the particular biomolecule and attachment site/strategy. In our experiment with spin-labeled DNA in trehalose, perhaps spirocyclohexane-substituted label is better immobilized compared to free **2c** in trehalose. The same happens to tetramethyl-substituted label, but only using a shorter, more rigid linker. We cannot provide an exhaustive explanation why such a noticeable difference in T_m of spirocyclohexane- and tetramethyl-substituted labels (920 vs. 550 ns) was found in Ref.10. Lengthening of $\boldsymbol{T}_m$ in spirocyclohexane-substituted label [10] compared to our results on free **2**-type radicals in trehalose can possibly be ascribed to interaction of spirocyclohexyl groups with protein hindering the NO librations. Opposite trend (shortening of T_m) observed for **1**-type label [10] compared to corresponding radical studied by us here implies higher mobility of label compared to free radical in glassy trehalose. Regardless the exact reasons, our results clearly demonstrate that the

attachment to biomolecule (not the intrinsic relaxation property) is responsible for the difference in T_m observed for two types of labels in Ref.10.

Note also that despite T_m of spirocyclohexane-substituted label attached to DNA is slightly superior compared to that of tetramethyl-substituted one, T_1 is ca. two times longer in the former case, hindering faster sequence repetition rate and prolonging the accumulation time. In many situations this might compensate the benefit of longer T_m for DEER measurements. At the same time, long T_1 might be useful for relaxation enhancement or saturation-recovery methods. In this sense spirocyclopentane-substituted radicals (especially **3**) are superior in comparison with spirocyclohexane-substituted ones.

Table 2. Relaxation times measured for spin-labeled single/double-stranded DNA in trehalose at 298 K at X-band. The samples were degassed at $3.5 \cdot 10^{-9}$ bar for 24 h.

	T_m / ns	T_1 / μs
D1-pip-spNIT/spNIT	850	25
D1-pip-NIT/NIT	720	13
D1-NH-NIT/NIT	800	13

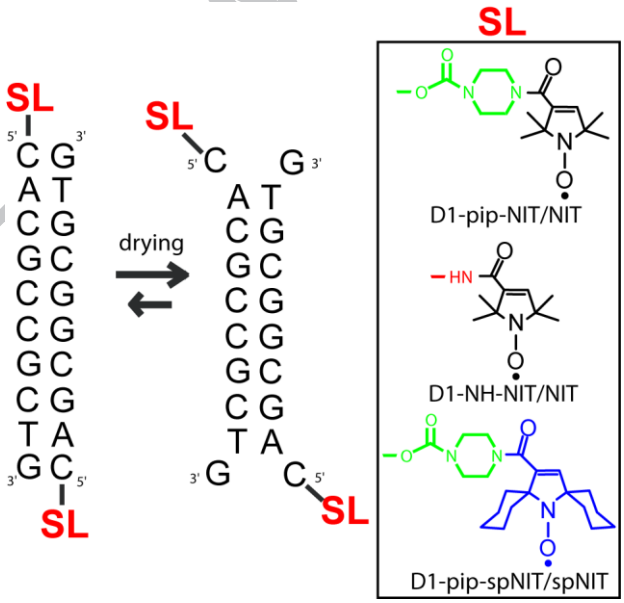

Figure 4. Structures of spin-labeled DNA duplexes.

III. Conclusions

Room-temperature pulse EPR distance measurements in biomolecules, being a long-standing goal since a few decades, are nowadays becoming more and more practical, owing to new types of spin labels used and/or new approaches of their immobilization, in particular using trehalose [10]. Being

motivated by a recent work of Eaton and colls.[10], we investigated a series of nitroxides with different substituents adjacent to NO-moiety as potential labels for room-temperature distance measurements. Surprisingly, we did not find sensible advantages in room-temperature relaxation properties of spirocyclohexane-substituted nitroxides immobilized in trehalose. At the same time, some differences in relaxation behavior between spirocyclohexane- and tetramethyl-substituted nitroxides arise when spin label is attached to biomolecule (in our case to 10-mer oligonucleotide). Therefore, our study shows that predicting room-temperature T_m values of spin-labeled biomolecules in glassy trehalose is more complicated than it was believed. In particular, specific interactions with biomolecule and spin labeling strategy might be more crucial than intrinsic relaxation properties of nitroxide. Another point to be considered for practical use is the stability of nitroxides in biological media, and tetraethyl-substituted radicals might be superior in this regard compared to tetramethyl- and spirocyclohexane-substituted ones [7, 29, 36]. Certainly, more studies are encouraged to provide systematization of various factors influencing ultimate T_m values and finding routes for long-range distance measurements at RT using nitroxides.

IV. Experimental Section

IV.1. Synthesis

We have synthesized 12 nitroxides **1**, **2a-d**, **3**, **4a,b**, **5a,b** and **6a,b** shown in Figure 1 below. The nitroxides **1** [37], **2a** [38], **2c** [29], **2d** [29], **3** [39], **4a** [40], **4b** [41], **5a** [42], **5b** [43] were prepared according to the literature protocols. Reagent grade MnO_2 (for catalysis) was used for oxidation. The IR spectra were acquired on an FT-IR spectrometer in KBr pellets (the concentration was 0.25%; the pellet thickness was 1 mm). The ^1H and ^{13}C NMR spectra were recorded on for 5-10% solutions at 300 K, using the signal of the solvent as the standard.

1,4,14,17-Tetraoxa-9-aza-21-oxotetraspiro[4.2.1.2.4.2.3.2]tetracos-9-yl-9-oxyl (**2b**) [44] was prepared in two steps from acetonine and 1,4-cyclohexanedione monoethylene acetal (Scheme 1) in analogy with the general methods described in Refs.44,45.

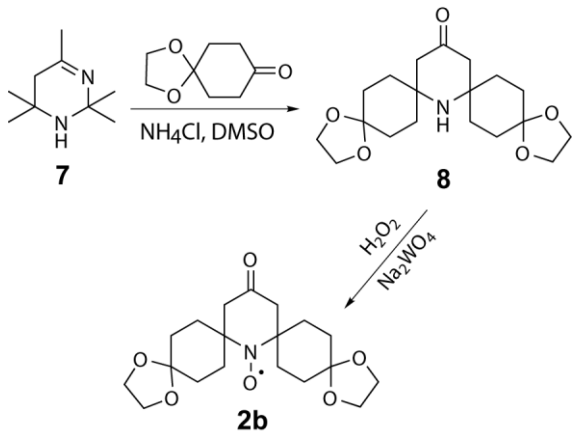

Scheme 1. Synthesis of **2b**.

1,4,14,17-Tetraoxa-9-azatetraspiro[4.2.1.2.413.210.38.25]tetracosan-21-one (**8**). A mixture of acetonin (**7**) monohydrate (4.5 g, 29 mmol), NH_4Cl (1.6 g, 29 mmol), 1,4-cyclohexanedione monoethylene acetal (27.2 g,174.3 mmol) and DMSO (20 mL) was stirred for 48 h at 60 °C under argon. The mixture was poured into water (200 mL) and acidified with CH_3COOH to pH about 6-5 and extracted with EtOAc (10 mL × 5). The water phase was basified to pH 10 using Na_2CO_3 and extracted with EtOAc (10 mL × 5). The extract was dried with Na_2CO_3 and the solvent was evaporated under reduced pressure. The residue was purified using column chromatography on silica gel (eluent chloroform) and crystallized from ether to give **8** (3.5 g, 35%). Mp 190-191 °C; ν_{max} (KBr)/cm^{-1} 3327, 3016, 2981, 2941, 2885, 2864, 1701, 1519, 1454, 1444, 1425, 1367, 1342, 1294, 1255, 1207, 1178, 1164, 1103, 1085, 1035, 1001, 981, 948, 933, 889, 862, 800, 769, 742, 665, 626, 607, 538, 486,435; ^{1}H NMR (300 MHz; $CDCl_3$) δ_H (ppm) 1.57-1.69 (12H, m), 1.86 (4H, m), 2.29 (4H, s), 3.89 (8H, t, $^3J_{H,H}$ = 2.1 Hz); ^{13}C NMR (75 MHz; $CDCl_3$) δ_C (ppm) 30.75 (CH_2), 37.47 (CH_2), 52.47 (C), 56.02 (CH_2), 64.03 (CH_2),64.05 (CH_2), 108.04 (C), 210.27 (C–O). The spectral data are very close to those reported in Ref.44.

1,4,14,17-Tetraoxa-9-aza-21-oxotetraspiro[4.2.1.2.4.2.3.2]tetracos-9-yl-9-oxyl (**2b**) was synthesized according modified published procedure [44]. A solution of Na_2WO_4×2 H_2O (0.3 g, 0.9 mmol) and EDTA disodium salt (0.3 g, 0.89 mmol) in water (5 ml) was poured into a solution of amine **8** (3 g, 8.5 mmol) in methanol (25 ml). Then 30% hydrogen peroxide (5 ml) was added and the solution was stored in a dark place at room temperature (20 °C) for 10 days. The methanol was distilled off under reduced pressure, the residue was extracted with chloroform, the chloroform solution was washed with 5% solution of $NaHSO_4$ and dried with Na_2CO_3. The solvent was distilled off under reduced pressure, the product was separated by column chromatography with $CHCl_3$ and recrystallized from hexane/ EtOAc to afford compound **2b** as an orange needles (2.2 g, 69%). mp 182-183 °C; ν_{max} (KBr)/cm^{-1} 2987, 2974, 2951, 2933, 2885, 2866, 1726, 1716, 1454, 1367, 1325, 1305, 1267, 1234, 1213, 1172, 1161, 1107, 1093, 1060, 1037, 1001, 979, 939, 898, 825, 754, 677, 661, 640, 528, 514, 482, 439.

The nitroxides **6a** and **6b** were prepared according to the Scheme 2.

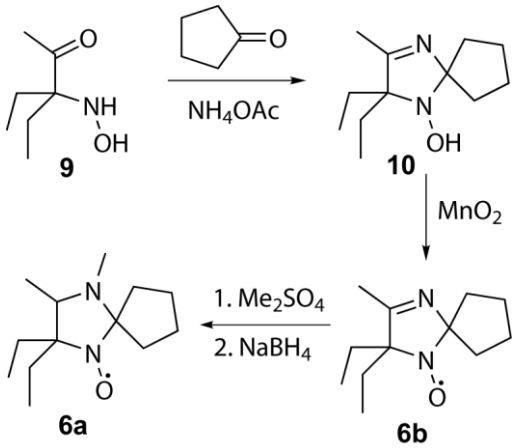

Scheme 2. Synthesis of **6a,b**.

2,2-Diethyl-3-methyl-1,4-diazaspiro[4,4]non-3-en-1-ol (10). A suspension of 3-hydroxyamino-3-ethylpentan-2-one hydrochloride **9** [40] (5 g, 27.5 mmol) and ammonium acetate (7.7 g, 100 mmol) in a mixture of cyclopentanone (10 mL, 93 mmol) and methanol (8 mL) was stirred under argon for 24 h. The resulting solution was poured into water (20 mL), basified with $NaHCO_3$, and extracted with diethyl ether (3 × 10 mL). The ether layers were thoroughly washed with water (5 × 10 mL) and dried over Na_2CO_3. The ether was removed under reduced pressure, the residue was triturated with hexane at -5 °C, and the crystalline precipitate of **10** was filtered off and washed with hexane, yielding 3.8 g, 65%, of colorless crystals, mp 111-115° C (hexane) (Found: C, 68.24; H, 10.55; N, 13.25. Calcd for $C_{12}H_{22}N_2O$: C, 68.53; H, 10.54; N, 13.32); ν_{max} (KBr)/cm^{-1} 2957, 2874, 2845, 1649, 1466, 1452, 1433, 1387, 1375, 1254, 1213, 1121, 1103, 1040, 1009, 986, 941, and 868; δH (500 MHz; $CDCl_3$) 0.80 (6 H, t, J = 7 Hz, 2 × CH_3, Et), 1,51 and 1.65 (each 2H, dq, J_d = 15 Hz, J_q = 7 Hz, CH_2, Et), 1.58, 1.66, 1.74 and 2.11 (each 2H, m, $(CH_2)_4$), 1.85 (3 H, s, CH_3C=N), and 5.44 (1 H, br s, OH); δC (125 MHz; $CDCl_3$) 9.1 (CH_3, Et), 16.9 (CH_3-C=N), 27.0 (CH_2, Et), 24.6 and 36.2 ($(CH_2)_4$), 78.0 (C5), 100.3 (C2), and 171.5 (C=N).

2,2-Diethyl-3-methyl-1,4-diazaspiro[4,4]non-3-en-1-oxyl (6b). Manganese dioxide (2 g, 23 mmol) was added to a stirred solution of **10** (1 g, 4.8 mmol) in chloroform (20 mL). The suspension was stirred for 0.5 h, manganese oxides were filtered off, and filtrate was evaporated under reduced pressure to leave orange liquid, which was purified by column chromatography on silica gel, eluent diethyl ether:hexane 1:20, to yield nitroxide **6b** (0.90 g, 90%), orange liquid, (Found: C, 69.09, H, 10.09; N, 13.28. Calcd for $C_{12}H_{21}N_2O$: C, 68.86; H, 10.11; N, 13.38); ν_{max} (neat)/cm^{-1} 2968, 2939, 2878, 1638, 1456, 1431, 1383, 1325, 1258, 1209, 1140, 1126, 1030, 1022, 988, 939 and 540.

2,2-Diethyl-3,4-dimethyl-1,4-diazaspiro[4,4]nonan-1-oxyl (6a). Dimethyl sulfate (0.5 g, 4 mmol) was added to a solution of **6b** (0.5 g, 2.4 mmol) in dry diethyl ether (3 mL). The solution was allowed to stand for 0.5 h at 25 °C and filtered, then diethyl ether was removed under reduced pressure. The residue was heated to 50 °C for 30 min under reduced pressure and then triturated with dry diethyl ether to form a highly hygroscopic yellow crystalline precipitate of quaternary salt. The precipitate was filtered off (without drying), washed with dry diethyl ether, and immediately dissolved in ethanol (5 mL). $NaBH_4$ (150 mg, 4 mmol) was added to the solution and the mixture was stirred for 1 h. Ethanol was removed under reduced pressure, and the residue was dissolved in water (2 mL) and extracted with diethyl ether (3 × 2 mL). The extract was dried over Na_2CO_3, then diethyl ether was removed under reduced pressure to leave a yellow oil, which was purified by column chromatography on silica gel, eluent diethyl ether:hexane 1:20, to yield the nitroxide **6b** (410 mg, 75%) as a yellow oil (Found: C, 69.22; H, 11.28; N, 12.43. Calcd for $C_{13}H_{25}N_2O$: C,

68.98; H, 11.58; N, 12.38); ν_{max} (neat)/cm^{-1} 2966, 2941, 2874, 2845, 2791, 1458, 1433, 1383, 1321, 1252, 1230, 1167, 1123, 1093, 1066, 1038, 995, 949, 923, 885, 849, and 507.

Synthesis of spin-labeled DNA. Synthesis of DNA spin-labeled by nitroxide **1** using NH- and piperazine type linkers is described in Ref.32. Synthesis of DNA spin-labeled by nitroxide **2c** using piperazine linker was done analogously [32], where N-hydroxysuccinimidic ether of nitroxide **2c** was used for spin-labeling.

IV.2. Sample preparation

All studied nitroxides were prepared in glassy trehalose (purchased from Sigma Aldrich and used as received) by means of lyophilization. Water solution of radical and 0.8 M trehalose in 1.5 ml Eppendorf tube was shock-frozen in liquid nitrogen, quickly transferred to the dessiccator and dried under vacuum for two hours. The concentration of radicals was adjusted to avoid spin-spin interactions between neighboring radicals in the dried sample (see Supporting Information). Below 0.05 mM (in initial solution) the dependence of T_m on concentration became insignificant; therefore such concentration was used as a tradeoff between reasonable signal intensity and small influence on T_m.

The samples were placed into quartz tubes (OD 3.8 mm, ID 2.8 mm for X-band and OD 2.8 mm, ID 1.8 mm for Q-band) and dried in two steps in order to investigate the influence of dehydration on relaxation times obtained. First samples were evacuated using forepump (10^{-3} bar) for two hours, as mentioned above. For deeper dehydration, samples were further evacuated at RT using turbomolecular pump ($3.5{\cdot}10^{-9}$ bar) for 24 hours. The splitter was connected directly to the head of the TMP. Commercial vacuummeter (Pfeiffer vacuum DPG 101) was connected to one of the outputs of the splitter. The sample tube was connected to the other output of the splitter via vacuum hose. Such design insured that the pressure measured by vacuummeter is closely the same as that in the sample tube, and test experiments evidenced that any leakage was directly detected by vacuummeter.

IV.3. EPR measurements

Continuous wave (CW) EPR measurements were carried out using commercial X-band spectrometer Bruker EMX. The CW EPR spectra were simulated using EasySpin [46]. Pulse EPR experiments were carried out using commercial X/Q-band Bruker Elexsys E580 spectrometer equipped with an Oxford flow helium cryostat and temperature control system. ER 4118X-MD5W and ER 5106QT resonators were used for X- and Q-band measurements, respectively. T_m was measured using a two-pulse electron spin echo (ESE) sequence; T_1 was measured using inversion-

recovery technique with inversion π-pulse and detecting two-pulse ESE sequence. Unless indicated otherwise, the π-pulse lengths were 20 and 100 ns at X/Q-band, respectively.

Acknowledgement

This work was supported by Russian Science Foundation (No. 14-14-00922). Synthesis of **2b** was performed with the support of RFBR (No. 15-03-04980).

References

[1] O. Duss, E. Michel, M. Yulikov, M. Schubert, G. Jeschke, F. H. T. Allain, Structural Basis of the Non-Coding RNA RsmZ Acting as a Protein Sponge, Nature 509 (2014) 588-592.

[2] O. Duss, M. Yulikov, G. Jeschke, F. H. T. Allain, EPR-aided approach for solution structure determination of large RNAs or protein-RNA complexes, Nature Comm. 5 (2014) 3669.

[3] G. Jeschke, DEER Distance Measurements on Proteins, Annu. Rev. Phys. Chem. 63 (2012) 419-446.

[4] P. P. Borbat,; J. H. Freed, Pulse Dipolar Electron Spin Resonance: Distance Measurements, Struct. Bonding (Berlin, Ger.) 2013, 1-82.

[5] O. Schiemann, T. F. Prisner, Long-Range Distance Determinations in Biomacromolecules by EPR Spectroscopy, Q. Rev. Biophys. 40 (2007) 1-53.

[6] Yu. D. Tsvetkov, Yu. A. Grishin, Techniques for EPR Spectroscopy of Pulsed Electron Double Resonance (PELDOR): A Review, Instrum. Exp. Technol. 52 (2009) 615-636.

[7] E. G. Bagryanskaya, O. A. Krumkacheva, M. V. Fedin, S. R. A. Marque, Development and Application of Spin Traps, Spin Probes, and Spin Labels, Methods Enzymol. 563 (2015), 365-396.

[8] Z. Y. Yang, Y. P. Liu, P. Borbat, J. L. Zweier, J. H. Freed, W. L. Hubbell, Pulsed ESR Dipolar Spectroscopy for Distance Measurements in Immobilized Spin Labeled Proteins in Liquid Solution, J. Am. Chem. Soc. 134 (2012) 9950-9952.

[9] G. Yu. Shevelev, O. A. Krumkacheva, A. A. Kuzhelev, A. A. Lomzov, O. Yu. Rogozhnikova, D. V. Trukhin, T. I. Troitskaya, V. M. Tormyshev, M. V. Fedin, D. V. Pyshnyi, E. G. Bagryanskaya, Physiological-Temperature Distance Measurement in Nucleic Acid using Triarylmethyl-Based Spin Labels and Pulsed Dipolar EPR Spectroscopy, J. Am. Chem. Soc. 136 (2014) 9874-9877.

[10] V. Meyer, M. A. Swanson, L. J. Clouston, P. J. Boratynski, R. A. Stein, H. S. Mchaourab, A. Rajca, S. S. Eaton, G. R. Eaton, Room-Temperature Distance Measurements of Immobilized Spin-Labeled Protein by DEER/PELDOR, Biophys. J. 108 (2015) 1213-1219.

[11] A. D. Milov, K. M. Salikhov, M. D. Shirov, Application of the Double Resonance Method to Electron Spin Echo in a Study of the Spatial Distribution of Paramagnetic Centers in Solids, Fiz. Tverd. Tela 23 (1981) 975-982.

[12] R. G. Larsen, D. J. Singel, Double Electron-Electron Resonance Spin-Echo Modulation - Spectroscopic Measurement of Electron-Spin Pair Separations in Orientationally Disordered Solids, J. Chem. Phys. 98 (1993) 5134-5146.

[13] M. Pannier, S. Veit, A. Godt, G. Jeschke, H. W. Spiess, Dead-Time Free Measurement of Dipole-Dipole Interactions Between Electron Spins, J. Magn. Reson. 142 (2000) 331-340.

[14] P. P. Borbat, H. S. Mchaourab, J. H. Freed, Protein Structure Determination Using Long-Distance Constraints from Double- Quantum Coherence ESR: Study of T4 lysozyme, J. Am. Chem. Soc. 124 (2002) 5304-5314.

[15] S. Saxena, J. H. Freed, Theory of Double Quantum Two-Dimensional Electron Spin Resonance with Application to Distance Measurements, J. Chem. Phys. 107 (1997) 1317-1340.

[16] V. V. Kurshev, A. M. Raitsimring, Yu. D. Tsvetkov, Selection of Dipolar Interaction by the 2+1 Pulse Train ESE, J. Magn. Reson. 81 (1989) 441-454.

[17] G. Jeschke, M. Pannier, A. Godt, H. W. Spiess, Dipolar Spectroscopy and Spin Alignment in Electron Paramagnetic Resonance, Chem. Phys. Lett. 331 (2000) 243.

[18] L. V. Kulik, S. A. Dzuba, I. A. Grigoryev, Yu. D. Tsvetkov, Electron Dipole-Dipole Interaction in ESEEM of Nitroxide Biradicals, Chem. Phys. Lett. 343 (2001) 315-324.

[19] S. Milikisyants, F. Scarpelli, M. G. Finiguerra, M. Ubbink, M. Huber, A Pulsed EPR Method to Determine Distances Between Paramagnetic Centers with Strong Spectral Anisotropy and Radicals: the Dead-Time Free RIDME Sequence, J. Magn. Reson. 201 (2009) 48-56.

[20] S. Razzaghi, M. Qi, A. I. Nalepa, A. Godt, G. Jeschke, A. Savitsky, M. Yulikov, RIDME Spectroscopy with Gd(III) Centers, J. Phys. Chem. Lett. 5 (2014) 3970-3975.

[21] A. Rajca, V. Kathirvelu, S. K. Roy, M. Pink, S. Rajca, S. Sarkar, S. S. Eaton, G. R. Eaton, A Spirocyclohexyl Nitroxide Amino Acid Spin Label for Pulsed EPR Spectroscopy Distance Measurements, Chem. Eur. J. 16 (2010) 5778-5782.

[22] V. Kathirvelu, C. Smith, C. Parks, Md. A. Mannan, Y. Miura, K. Takeshita, S. S. Eaton, G. R. Eaton, Relaxation Rates for Spirocyclohexyl Nitroxyl Radicals are Suitable for Interspin Distance Measurements at Temperatures up to about 125 K, Chem. Commun. (2009) 454-456.

[23] A. Savitsky, M. Malferrari, F. Francia, G. Venturoli, K. Moebius, Bacterial Photosynthetic Reaction Centers in Trehalose Glasses: Coupling between Protein Conformational Dynamics and Electron-Transfer Kinetics as Studied by Laser-Flash and High-Field EPR Spectroscopies, J. Phys. Chem. B 114 (2010) 12729-12743.

[24] M. Malferrari, A. Nalepa, G. Venturolo, F. Francia, W. Lubitz, K. Mobius, A. Savitsky, Structural and dynamical chacteristics of trehalose and sucrose matrices at different hydration levels as probed by FRIR and high-field EPR, Phys.Chem.Chem.Phys. 16 (2014), 9831-9848

[25] K. Mobius, A. Savitsky, A. Nalepa, M. Malferrari, F. Francia, W. Lubitz, W. Lubitz, G. Venturolo, The Magic of Disaccharide Glass Matrices for Protein Function as Decoded by High-Field EPR and FTIR Spectroscopy, Appl. Magn. Res. 46 (2015) 435-464.

[26] E. P. Kirilina, S. A. Dzuba, A. G. Maryasov, Yu. D. Tsvetkov, Librational Dynamics of Nitroxide Molecules in a Molecular Glass Studied by Echo-Detected EPR, Appl. Magn. Reson. 21 (2001) 203-221.

[27] A.Barbon, M. Brustolon, Maniero, A. L. Romanelli, M. Brunel, Dynamics and Spin Relaxation of Tempone in a Host Crystal. An ENDOR, High Field EPR and Electron Spin Echo Study, Phys. Chem. Chem.Phys., 1 (1999) 4015-4023K.

[28] A. Zecevic, G. R. Eaton, S. S. Eaton and M. Lindgren, Dephasing of Electron Spin Echoes for Nitroxyl Radicals in Glassy Solvents by Non-methyl and Methyl Protons, Mol. Phys., 95 (1998) 1255-1263.

[29] I. A. Kirilyuk, Yu. F. Polienko, O. A. Krumkacheva, R. K. Strizhakov, Yu. V. Gatilov, I. A. Grigor'ev, E. G. Bagryanskaya, Synthesis of 2,5-Bis(spirocyclohexane)-Substituted Nitroxides of Pyrroline and Pyrrolidine Series, Including Thiol-Specific Spin Label: An Analogue of MTSSL with Long Relaxation Time, J. Org. Chem. 77 (2012) 8016-8027.

[30] H. Sato , V. Kathirvelu , A. Fielding, J. P. Blinco, A. S. Micallef, S. E. Bottle, S. S. Eaton, G. R. Eaton, Impact of molecular size on electron spin relaxation rates of nitroxyl radicals in glassy solvents between 100 and 300 K, Mol. Phys. 105 (2007) 2137–2151.

[31] J. R. Biller, H. Elajaili, V. Meyer, G. M. Rosen, S. S. Eaton, G. R. Eaton, Electron spin–lattice relaxation mechanisms of rapidly-tumbling nitroxide radicals, J. Magn. Reson. 236 (2013) 47-56.

[32] G. Yu. Shevelev, O. A. Krumkacheva, A. A. Lomzov, A. A. Kuzhelev, D. V. Trukhin, O. Yu. Rogozhnikova, V. M. Tormyshev, D. V. Pyshnyi, M. V. Fedin, E. G. Bagryanskaya, Triarylmethyl Labels: Toward Improving the Accuracy of EPR Nanoscale Distance Measurements in DNAs, J. Phys. Chem. B 119 (2015) 13641−13648.

[33] A.-N. Spiess, N. Mueller, R. Ivell, Trehalose Is a Potent PCR Enhancer: Lowering of DNA Melting Temperature and Thermal Stabilization of *Taq* Polymerase by the Disaccharide Trehalose, Clin. Chem. 50 (2004) 1256-1259.

[34] M. Marušič, H. Tateishi-Karimata, N. Sugimoto, Janez Plavec, Structural foundation for DNA behavior in hydrated ionic liquid: An NMR study, Biochimie 108 (2015) 169-177.

[35] M. Zgarbová, M. Otyepka, J. Šponer, F. Lankaš, P. Jurečka, Base Pair Fraying in Molecular Dynamics Simulations of DNA and RNA, J. Chem. Theory Comput. 10 (2014) 3177-3189.

[36] A. P. Jagtap, I. Krstic, N. C. Kunjir, R. Hansel, T. F. Prisner, S. Th. Sigurdsson, Sterically shielded spin labels for in-cell EPR spectroscopy: Analysis of stability in reducing environment, Free Rad. Res. 49 (2015) 78-85.

[37] E. G. Rozantsev, Free Nitroxyl Radicals; Ulrich, H., Ed.; Plenum Press: New York, 1970; p 249 (translated from Russian by B. J. Hazzard).

[38] Y. Miura, N. Nakamura, I. Taniguchi, Low-Temperature "living" Radical Polymerization of Styrene in the Presence of Nitroxides with Spiro Structures, Macromolecules 34 (2001) 447-455.

[39] D. A. Morozov, I. A. Kirilyuk, D. A. Komarov, A. Goti, I. Yu. Bagryanskaya, N. V. Kuratieva, I. A. Grigor'ev, Synthesis of a Chiral C2-Symmetric Sterically Hindered Pyrrolidine Nitroxide Radical via Combined Iterative Nucleophilic Additions and Intramolecular 1,3-Dipolar Cycloadditions to Cyclic Nitrones, J. Org. Chem. 77 (2012) 10688-10698.

[40] I. A. Kirilyuk, A. A. Bobko, I. A. Grigor'ev, V. V. Khramtsov, Synthesis of the tetraethyl substituted pH-sensitive nitroxides of imidazoline series with enhanced stability towards reduction, Org. Biomol. Chem. 2 (2004) 1025-1030.

[41] A. A. Bobko, I. A. Kirilyuk, N. P. Gritsan, D. N. Polovyanenko, I. A. Grigor'ev, V. V. Khramtsov, E. G. Bagryanskaya, EPR and Quantum Chemical Studies of the pH-sensitive Imidazoline and Imidazolidine Nitroxides with Bulky Substituents, Appl. Magn. Reson. 39 (2010) 437-451.

[42] D. Zubenko, Yu. Tsentalovich, N. Lebedeva, I. Kirilyuk, G. Roshchupkina, I. Zhurko, V. Reznikov, S. R. A. Marque, E. Bagryanskaya, Laser Flash Photolysis and CIDNP Studies of Steric Effects on Coupling Rate Constants of Imidazolidine Nitroxide with Carbon-Centered Radicals, Methyl Isobutyrate-2-yl and *tert*-Butyl Propionate-2-yl, J. Org. Chem. 71 (2006) 6044-6052.

[43] A. A. Bobko, I. A. Kirilyuk, I. A. Grigor'ev, J. L. Zweier, V. V. Khramtsov, Reversible Reduction of Nitroxides to Hydroxylamines: Roles for Ascorbate and Glutathione. Free Radic. Biol. Med. 42 (2007) 404-412.

[44] K. Sakai, K. Yamada, T. Yamasaki, Y. Kinoshita, F. Mito, H. Utsumi, Effective 2,6-substitution of Piperidine Nitroxyl Radical by Carbonyl Compound, Tetrahedron 66 (2010) 2311-2315.

[45] Yu. Kinoshita, K. Yamada, T. Yamasaki. H. Sadsue. K. Sakai. H. Utsumi, Development of Novel Nitroxyl Radicals for Controlling Reactivity with Ascorbic Acid, Free Rad. Res. 43 (2009) 565-571.

[46] S. Stoll, A. Schweiger, Easyspin, a Comprehensive Software Package for Spectral Simulation and Analysis in EPR., J. Magn. Reson. 178 (2006) 42-55.

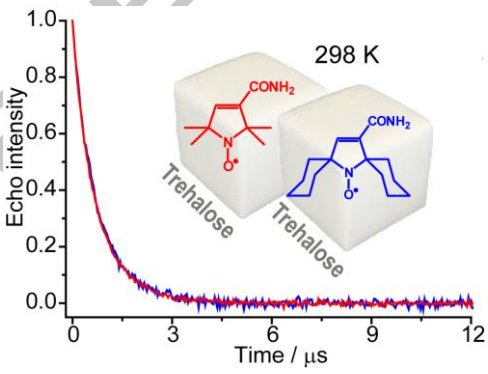

TOC graphic

Being motivated by a recent work of Eaton and colls.[Biophys. J. 108 (2015) 1213-1219], we investigated a series of nitroxides with different substituents adjacent to NO-moiety including spirocyclohexane, cyclopentane, tetraethyl and tetramethyl groups as potential labels for room-temperature distance measurements. Electron spin relaxation times (T_1, T_m) were measured at room temperature at X- and Q-bands (9/34 GHz) and a comparison was made with the corresponding relaxation times in nitroxide-labeled DNA immobilized in trehalose. Surprisingly, we did not find sensible advantages in room-temperature relaxation properties of spirocyclohexane-substituted nitroxides immobilized in trehalose. Therefore, unless there are specific interactions between spin labels and biomolecules, the room-temperature value of T_m in trehalose is weakly dependent on the structure of substituents adjacent to NO-moiety of nitroxide. The issues of specific interactions and stability of nitroxide labels in biological media might be more important for room temperature pulsed dipolar EPR than differences in intrinsic spin relaxation of radicals.

.